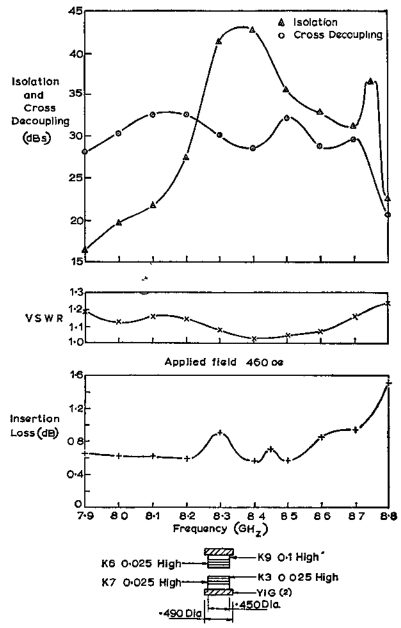

(a). Performance of YIG (2) with constant-diameter dielectric disks.

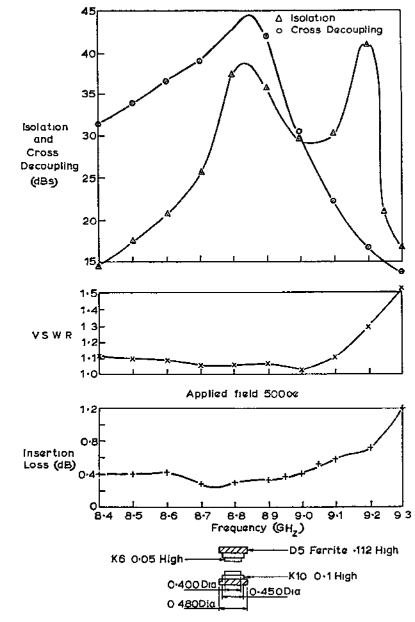

(c). An improved bandwidth is obtained for D5 ferrite by varying the dielectric geometric structure.

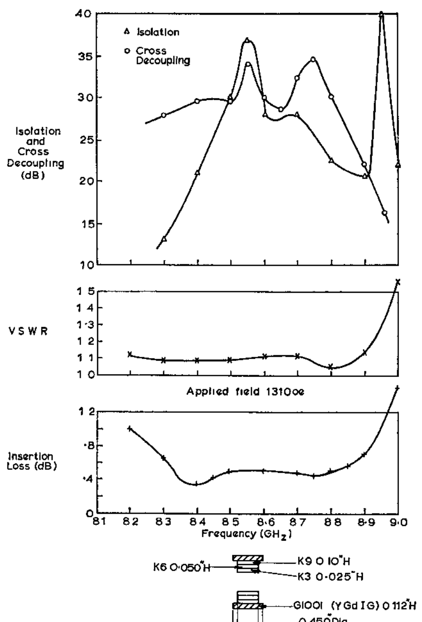

(b). Performance of YGdIG with constant-diameter dielectric disks, showing the decreased insertion loss compared with Fig. 4(a).

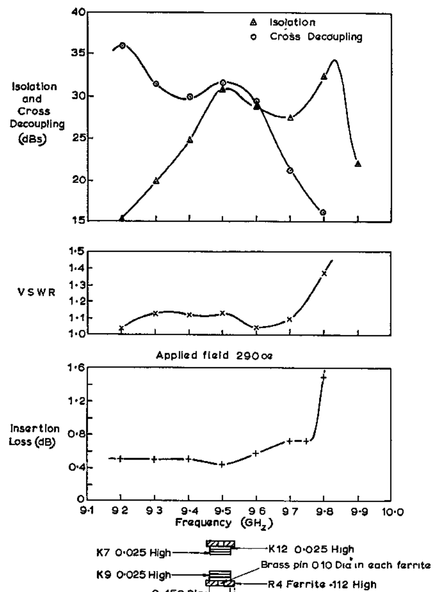

(d). Typical example of the change in frequency produced by the introduction of a conducting pin into the ferrite (R4).

Fig. 4.

the waveguide has proved difficult but two methods have been tried. The first was to use ferrite with a central conducting pin [Fig. 4(d)]. Here the operating bandwidth has been shifted up to 500 MHz with a conducting pin of 0.10-inch diameter. Larger-diameter pin sizes have resulted in increased insertion loss. The other method of increasing the frequency was to reduce the height of the junction by the introduction of conducting disks under the ferrite. The bandwidth shifted only slowly with relatively large conducting disks.

The E-plane circulator geometry is less liable to breakdown than an H-plane device; we have observed no breakdown up to power levels of at least 60 kW peak. The isolation characteristics are unchanged with all the materials examined at these power levels. There is, however, an increase in insertion loss with power level; the material with the lowest increase is manganese-aluminum ferrite (Ferroxcube 5B1), with a saturation magnetization of 1045 gauss. This circulator handled a mean power of 40 watts with a duty cycle of 0.001, and gave the following performance at 9.0 GHz:

Isolation	1–4	>20 dB
Isolation	1–3	>20 dB
Insertion loss	1–2	<0.7 dB
VSWR		1.13.

This circulator is compact and some improvement in insertion loss can be expected with better materials. Larger bandwidths appear possible with variation on the previously mentioned matching techniques.

S. R. Longley[3]
Mullard Research Labs.
Redhill, Surrey, England

[3] Mr. Longley is now engaged in postgraduate studies at University College, London.

Gap Spacing for End-Coupled and Side-Coupled Strip-Line Filters

Two of the simplest strip-line configurations for bandpass filters are those which utilize end coupling [1], [2] (Fig. 1) and side coupling [3] (Fig. 2). For the special case of a symmetric strip line with center conductor of negligible thickness (Fig. 3), it is possible to establish expressions which explicitly relate gap spacing S to normalized bandwidth w. Generally it is found that the greater the gap width, the less important are the tolerance considerations; alternatively, a broader bandwidth may be achieved for a given tolerance. The purpose of this correspondence is to establish a criterion that will enable a designer to select the filter with the greater coupling gap for given values of ground plane spacing D, midband wavelength λ_0, and normalized bandwidth.

The equivalent circuit of a series gap in an end-coupled filter (center-line representation) comprises a series capacitance C_1 and two shunt capacitances C_2 (Fig. 4). Approximate analytic relations are available [4] which relate the normalized susceptances associated with C_1 and C_2 to S, D, and λ_0' $(=\lambda_0/\sqrt{\epsilon_r})$:

$$b_1 = \frac{D}{\lambda_0'} \ln \left\{ \coth \left(\frac{\pi}{2} \cdot \frac{S}{D} \right) \right\} \quad (1)$$

$$b_2 = \frac{-2D}{\lambda_0'} \ln \left\{ \cosh \left(\frac{\pi}{2} \cdot \frac{S}{D} \right) \right\}. \quad (2)$$

Equations (1) and (2) are valid for $W/D > 0.35$ and $T/D < 0.1$. Experimental evidence for their accuracy has been obtained by Oliner [5], where b_1 and b_2 are plotted as a function of S/W. As S/D decreases, b_1 rapidly rises (theoretically to infinity) while b_2 slowly decreases (theoretically to zero). In particular, for $S/D < 0.2$, $b_1 > 10\,|b_2|$, and for $S/D < 0.1$, $b_1 > 100\,|b_2|$. Assuming that S/D is sufficiently small, b_2 can be neglected and the analysis that follows is considerably simplified.

The normalized susceptance of the $(i+1)$th gap of an end-coupled filter with n stages,

Manuscript received November 28, 1966.

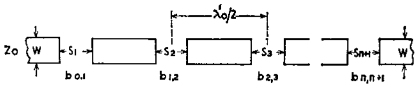

Fig. 1. Half-wavelength end-coupled filter.

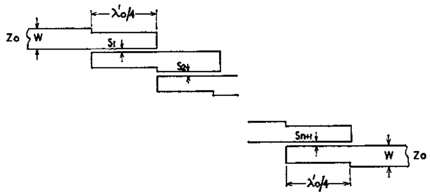

Fig. 2. Half-wavelength side-coupled filter.

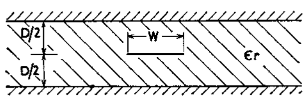

Fig. 3. Cross section of symmetric strip line.

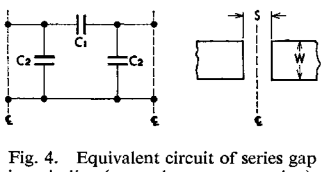

Fig. 4. Equivalent circuit of series gap in strip line (center-line representation).

$b_{i,i+1}$ has been given by various authors [1], [2] and can be expressed in the following way:

$$b_{i,i+1} = \chi_{i,i+1}/(1 - \chi^2_{i,i+1}) \qquad (3)$$

where

$$\chi_{0,1} = \sqrt{\frac{\pi w}{2 g_0 g_1}} = \chi_{n,n+1} \qquad (4)$$

$$\chi_{i,i+1} = \frac{\pi w}{2\sqrt{g_i g_{i+1}}} \text{ for } (n-1) \geq i \geq 1 \qquad (5)$$

$w = (f_2 - f_1)/f_0$

= normalized bandwidth

g = normalized value of lowpass prototype element.

Equation (1) can be rearranged into a form in which S/D is expressed as a function of susceptance:

$$\frac{S}{D} = \frac{1}{\pi} \ln \left\{ \coth \left(\frac{b_1 \lambda_0'}{2D} \right) \right\}. \qquad (6)$$

Substituting for b_1 from (3), omitting the i subscripts, and replacing λ_0' by $\lambda_0/\sqrt{\epsilon_r}$ modifies (6) to become

$$\frac{S}{D} = \frac{1}{\pi} \ln \left[\coth \left\{ \frac{\lambda_0}{2\sqrt{\epsilon_r} D} \cdot \frac{\chi}{1 - \chi^2} \right\} \right]. \qquad (7)$$

An explicit expression for S/D in terms of χ has now been established for end-coupled filters and permits comparison with an equivalent expression for side-coupled filters which can now be derived. The appropriate design equations for side-coupled filters have been given by Cohn [3] and can be expressed as follows:

$$\left(\frac{Z_{0e}}{Z_0}\right)_{i,i+1} = 1 + \chi_{i,i+1} + \chi^2_{i,i+1} \qquad (8)$$

$$\left(\frac{Z_{0o}}{Z_0}\right)_{i,i+1} = 1 - \chi_{i,i+1} + \chi^2_{i,i+1} \qquad (9)$$

where Z_{0e} and Z_{0o} are the even- and odd-mode impedances, respectively, and Z_0 is the characteristic impedance with $i=0$ to $i=n$. Explicit relations for Z_{0e} and Z_{0o} in terms of W/D, S/D, and ϵ_r have also been derived by Cohn [6]. Rearranged they are

$$Z_{0e} = \frac{94.15/\sqrt{\epsilon_r}}{\frac{W}{D} + \frac{\ln 2}{\pi} + \frac{1}{\pi} \ln \left\{ 1 + \tanh \left(\frac{\pi}{2} \cdot \frac{S}{D} \right) \right\}} \qquad (10)$$

$$Z_{0o} = \frac{94.15/\sqrt{\epsilon_r}}{\frac{W}{D} + \frac{\ln 2}{\pi} + \frac{1}{\pi} \ln \left\{ 1 + \coth \left(\frac{\pi}{2} \cdot \frac{S}{D} \right) \right\}}. \qquad (11)$$

Equations (10) and (11) are accurate to ~1 percent for $W/D \geq 0.35$.

Eliminating W/D from (10) and (11), substituting for Z_{0e} and Z_{0o} from (8) and (9), and dropping the i subscripts yields

$$\frac{1}{\pi} \ln \left\{ \tanh \left(\frac{\pi}{2} \cdot \frac{S}{D} \right) \right\} = \frac{-188.3}{\sqrt{\epsilon_r} Z_0} \cdot \frac{\chi(1 - \chi^2)}{(1 - \chi^6)}. \qquad (12)$$

Equation (12) can now be rearranged as an explicit function of S/D:

$$\frac{S}{D} = \frac{1}{\pi} \ln \left[\coth \left\{ \frac{94.15\pi}{\sqrt{\epsilon_r} Z_0} \cdot \frac{\chi(1 - \chi^2)}{(1 - \chi^6)} \right\} \right]. \qquad (13)$$

Upon examining the arguments of the hyperbolic cotangent functions, one sees (7) and (13) to be closely similar in form. If $\chi \ll 1$, higher terms in χ can be neglected with negligible loss in accuracy, and it is readily seen that (7) and (13) become identical, provided that

$$\frac{\lambda_0}{2D} = \frac{94.15\pi}{Z_0}. \qquad (14)$$

For a 50 Ω line, which is a typical requirement in practice, (14) can be simplified to yield

$$\frac{\lambda_0}{D} \approx 12. \qquad (15)$$

From (15), in conjunction with the simplified forms of (7) and (13), it can be concluded that the coupling gaps for side-coupled filters will be greater than those for end-coupled filters, if $\lambda_0 > 12D$. For $\lambda_0 < 12D$, the gaps can be expected to be greater for the end-coupled configuration, which may consequently be the preferred form. These two conclusions apply only for $Z_0 = 50$ Ω. For lines of differing characteristic impedance, λ_0/D will change, decreasing to approximately 8 for $Z_0 = 75$ Ω. Consequently, an increase in Z_0 for a given $\lambda_0 | D$ will extend the range for which side-coupled filters give smaller gap spacings.

A more accurate assessment of filter type can be determined by considering all the χ terms in (7) and (13). Equation (14) is modified with the following result:

$$\frac{\lambda_0}{D} = \frac{188.3\pi}{Z_0} \cdot \frac{(1 - \chi^2)^2}{(1 - \chi^6)}. \qquad (16)$$

The numerical range of values which χ can assume may be evaluated by examining (4) and (5), (8) and (9). The two formulas in (4) and (5) show that w is directly proportional to χ^2 for $i=0$ and $i=n$, but proportional only to χ for all other permitted values of i. As b is related to χ in (3) and to S/D in (1), it is readily perceived that changes in gap width for the first and last stages of an end-coupled filter will have a greater effect on w than will any other stage, a fact that has been well established by experiment. Moreover, it is evident from (7) that S/D will be less for the first and last stages than for the others, as χ is greater for $i=0$ and $i=n$ than for $(n-1) \geq i \geq 1$. This conclusion has also been substantiated by experiment. Consequently, the coupling gap of only the first stage need be considered in assessing the smallest required gap, and hence the most critical one as far as bandwidth is concerned.

A similar argument shows that the conclusions of the previous paragraph also apply to side-coupled filters. Figure 4 in Cohn [6] is a graph of Z_{0e} and Z_{0o} versus W/D and S/D from which it is apparent that both impedances are monotonic functions for $S/D \geq 0.01$ and $3.0 \geq W/D \geq 0.1$. However, in (9) Z_{0o} changes monotonically with χ over any range that does not include $\chi = 0.5$. Consequently, to use (8) and (9) with (10) and (11) in a way that is mathematically consistent, χ must never exceed 0.5 if the value $\chi = 0$ is to be included. Furthermore, by considering (4), a value of χ as high as 0.5 can still correspond to values of w for which (3) and (4), (8) and (9) are said to be accurate [1], [2]. For a maximally flat response, $g_0 = 1$ and $g_1 = 2 \sin(\pi/2n)$ [1]–[3].

Substituting for g_0 and g_1 in (4) and rearranging terms, one can express w as a function of χ:

$$w = \frac{4}{\pi} \chi^2 \sin \left(\frac{\pi}{2n} \right). \qquad (17)$$

If $\chi = 0.5$ and $n \geq 2$, w will never exceed 0.21. In Cohn [3] it is stated that bandwidths as great as 20 percent are possible for a maximally flat response, which is consistent with χ having a value as great as 0.5. A similar argument can be used for the case of an equal-ripple response. Substituting $\chi = 0.5$ in (17), putting $Z_0 = 50$ Ω, and simplifying, one obtains a further approximation for λ_0/D which supplements (15):

$$\frac{\lambda_0}{D} \approx 7. \qquad (18)$$

Hence, for $\lambda_0 > 12D$, side-coupled filters will always have larger coupling gaps; for $\lambda_0 < 7D$, end-coupled filters will have greater gap spacings. The conclusions presuppose the stated range of values of S/D, W/D, and w for $Z_0 = 50$ Ω. For $12D > \lambda_0 > 7D$, it is necessary to determine χ from (4) and substitute its value in (16). If λ_0/D is greater than the right-hand side of (16), side coupling is preferable; if λ_0/D is less, then end coupling will give larger gaps.

Finally, in a practical design it is usually necessary that

$$\frac{\lambda_0'}{2} > D \tag{19}$$

in order to prevent the generation of TM modes [7] and so minimize loss by radiation. By rearranging (19) and replacing λ_0' by $\lambda_0/\sqrt{\epsilon_r}$, one imposes a further constraint on the permissible range of the λ_0/D ratio for end-coupled filters and for all values of characteristic impedance:

$$\frac{\lambda_0}{D} > 2\sqrt{\epsilon_r}. \tag{20}$$

To facilitate selection of the filter type, a graph has been prepared with λ_0'/D as a function of $\sqrt{\epsilon_r}\, Z_0$ (Fig. 5), incorporating (14), (16), and (20).

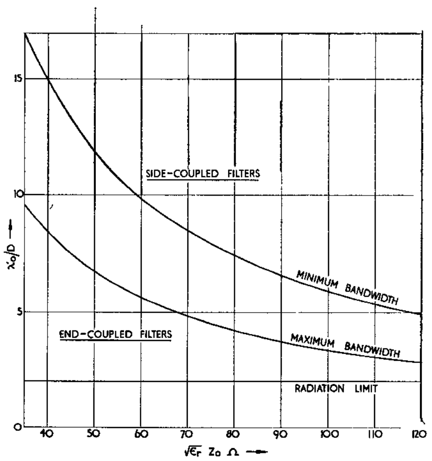

Fig. 5. λ_0'/D as a function of $\sqrt{\epsilon_r}Z_0$ for complete bandwidth range.

ACKNOWLEDGMENT

The permission of the Australian Post Office Research Laboratories to publish this correspondence is acknowledged.

J. K. Richardson
Microwave Techniques Div.
P.M.G. Research Labs.
Melbourne, Australia

REFERENCES

[1] S. B. Cohn, "Direct-coupled-resonator filters," *Proc. IRE*, vol. 45, pp. 187–196, February 1957.
[2] E. H. Bradley, "Design and development of strip-line filters," *IRE Trans. on Microwave Theory and Techniques*, vol. MTT-4, pp. 86–93, April 1956.
[3] S. B. Cohn, "Parallel coupled strip line resonator filters," *Onde Elec.* (*France*), pp. 140–146, October 1957.
[4] H. M. Altschuler and A. A. Oliner, "Discontinuities in the Center Conductor of Symmetric Strip Transmission Line," *IRE Trans. on Microwave Theory and Techniques*, vol. MTT-8, pp. 328–339, May 1960.
[5] A. A. Oliner, "Equivalent circuits for discontinuities in balanced strip transmission line," *IRE Trans. on Microwave Theory and Techniques*, vol. MTT-3, pp. 134–143, March 1955.
[6] S. B. Cohn, "Shielded coupled-strip transmission line," *IRE Trans. on Microwave Theory and Techniques*, vol. MTT-3, pp. 29–38, October 1955.
[7] K. S. Packard, "Optimum impedance and dimensions for strip transmission line," *IRE Trans. on Microwave Theory and Techniques*, vol. MTT-5, pp. 244–247, October 1957.

An Interesting Impedance Matching Network

Any load impedance can be transformed to a real impedance by a $\lambda/8$ transformer whose characteristic impedance is equal to the magnitude of the load impedance.

The locus of a normalized load impedance, as a function of the characteristic impedance of the feed line, is a constant (X/R) contour on the Smith chart. Further, a constant (X/R) contour is a circular segment drawn through the points zero and infinity. The point of closest approach of any constant (X/R) contour to the $(Z/Z_0)=1$ point, minimum $|\Gamma|$, takes place along a straight line drawn from $(Z/Z_0)=j$ to $(Z/Z_0)=-j$, or $\lambda/8$ away from the real axis. Therefore, if any load is fed by a line whose characteristic impedance minimizes the magnitude of the reflection coefficient at the load, the normalized impedance $\lambda/8$ away from the load will be pure real.

Consider the matching network in Fig. 1.

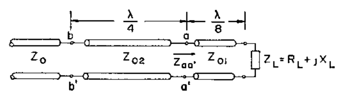

Fig. 1. Load-line impedance match.

The squared magnitude of the reflection coefficient at the load is given by

$$|\Gamma|^2 = \frac{|Z_L|^2 - 2R_LZ_{01} + Z_{01}^2}{|Z_L|^2 + 2R_LZ_{01} + Z_{01}^2} \tag{1}$$

where

$$R_L = \text{Re}\,\{Z_L\}.$$

We may write

$$|\Gamma|^2 = 1 - \delta \tag{2}$$

where

$$\delta = \frac{4R_LZ_{01}}{|Z_L|^2 + 2R_LZ_{01} + Z_{01}^2}. \tag{3}$$

Then

$$\frac{\partial\delta}{\partial Z_{01}} = 0 \tag{4}$$

implies that

$$(|Z_L|^2 + 2R_LZ_{01} + Z_{01}^2)(4R_L) - (4R_LZ_{01})(2R_L + 2Z_{01}) = 0 \tag{5}$$

or

$$Z_{01}^2 = |Z_L|^2. \tag{6}$$

Therefore, $|\Gamma|^2$ is a minimum if $Z_{01} = |Z_L|$. Since $|\Gamma|<1$, $|\Gamma|$ will also be minimized by the same value of Z_{01}.

The driving point impedance of the $\lambda/8$ transformer, $Z_{aa'}$ in Fig. 1 is

$$Z_{aa'} = \frac{R_L}{1 - \dfrac{X_L}{|Z_L|}} \tag{7}$$

when

$$Z_{01} = |Z_L|.$$

Manuscript received December 5, 1966.

Thus if the Q of the load impedance is high,

$$Z_{aa'} \cong \begin{cases} \dfrac{R_L}{2}, & X_L < 0 \\ 2X_LQ_L, & X_L > 0 \end{cases} \tag{8}$$

where

$$Q_L = \frac{X_L}{R_L}. \tag{9}$$

The impedance of the quarter-wave transformer in Fig. 1 may then be found from

$$Z_{01} = \sqrt{Z_{aa'}Z_0} \tag{10}$$

as is well known.

By application of the same principles, a conjugate match between two impedances Z_G and Z_1 may be accomplished in a $\lambda/2$ length of line as shown in Fig. 2, where

$$Z_{01} = |Z_L| \tag{11}$$

$$Z_{02} = \left[\frac{R_LR_G|Z_L|\,|Z_G|}{(|Z_L| - X_L)(|Z_G| - X_G)}\right]^{1/2} \tag{12}$$

$$Z_{03} = |Z_G| \tag{13}$$

in which

$$Z_L = R_L + jX_L \tag{14}$$

$$Z_G = R_G + jX_G. \tag{15}$$

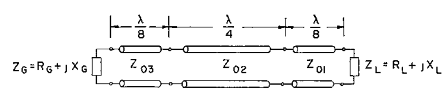

Fig. 2. Source-load impedance match.

These circuits do not constitute minimum length solutions to the impedance matching problem. They do provide a simple answer to the synthesis problem in cases where frequency response is not the primary concern, as is the case in many frequency multiplier design problems. In addition, the line lengths involved are always known in advance. This property has been found to be particularly useful in microwave circuit design when the exact value of the input impedance is not a priori known.

Donald H. Steinbrecher
M.I.T. Research Lab. of Electronics
Cambridge, Mass.

A Laminar Slow-Wave Coupler and Its Application to Indium Antimonide

The purpose of this correspondence is to describe a technique for coupling energy between a waveguide mode and a semiconductor (or gas discharge) slow wave that has a longitudinal component of microwave electric

Manuscript received January 3, 1967. The research reported here was sponsored by the Air Force Avionics Laboratory, Research and Technology Division, U. S. Air Force Systems Command, Wright-Patterson AFB, Ohio, under Contract AF-33(615)-1608, and by RCA Laboratories, Princeton, N. J.